

Slava V. Rotkin · Yury Gogotsi

## Analysis of non-planar graphitic structures: from arched edge planes of graphite crystals to nanotubes

Received: 29 October 2001 / Accepted: 5 November 2001

**Abstract** A unified approach to the analysis of the mechanisms that lead to the edge reconstruction of graphite and growth of a variety of non-planar graphitic structures, such as nanotubes, is suggested. Transmission electron microscopy (TEM) shows that nano-arches are formed on the edge planes of natural and synthetic graphite, as well as graphite polyhedral crystals, which are built of graphene sheets; this makes the edge reconstruction of graphite different from the surface reconstruction of other crystals. A theoretical study of edge zipping in graphite and formation of tubular carbon structures has been performed using an integrated approach combining molecular dynamics simulation and analytical continual energetics modeling. The suggested theoretical framework describes the formation of curved surfaces in a wide range of dimensions, which is a general feature of the growth of layered materials. Layered materials isostructural to graphite, such as hexagonal BN, demonstrate similar edge structures and also form nanotubes. Thus, the ability of materials to form arches as a result of edge reconstruction points out to their ability to form nanotubes and vice versa. TEM studies of graphite and hexagonal boron nitride provide experimental verification of our analytical model.

**Keywords** Graphite · Continual energetics · Molecular dynamics · Nanotube · Transmission electron microscopy · Edge reconstruction

### Introduction

Every field of engineering seems to have a favorite material. Steel is the most important material for mechani-

cal engineers. Silicon dominates in electronics. Nanotechnologists selected carbon from the beginning because of the fullerenes [1] and nanotubes [2], which have been considered objects on the size scale compatible with nanodevices. Carbon and carbon-based materials attract the attention of researchers not only because of their morphology and mechanical properties but also due to their unique electronic properties including high temperature superconductivity [3], rectifying behavior [4], and field effect transistors [5–7].

Conventional graphite forms hexagonal plate-like crystals (kish graphite) [8], with weak bonding between graphite layers. Most of the carbon materials produced at temperatures 1000–2000 °C have a disordered structure (carbon black, soot, glassy carbon and carbon fibers). Graphitization of solid carbon occurs at temperatures close to 3000 °C. Partial graphitization and the formation of polygons was observed after heat treatment of carbon black at 2800 °C [9]. However, making large crystals of graphite is extremely difficult and both natural and man-made crystals do not exceed several millimeters in size. Thus, large and perfect graphite crystals occur probably less frequently than large diamonds.

Graphite whiskers [10] and carbon nanotubes (NT) [11] represent unusual forms of  $sp^2$  carbon due to the distortion of their graphite sheets. In graphite whiskers, a graphite sheet (graphene) simply rolls into a scroll [10] and the layers have short and medium range order, but not the long-range periodicity of crystalline graphite. The discovery of single-wall nanotubes (SWNT), SWNT ropes, self-assembled SWNT single crystals [12], and multiwall carbon nanotubes (MWNT), consisting of coaxial closed or open tubes, demonstrated the existence of a variety of non-planar structures built of graphene sheets. Great interest in novel nanostructures, such as nanotubes, fullerenes and other nonplanar carbon allotropes, resulted in a decreasing interest in bulk planar graphite. In spite the fact that SWNTs, MWNTs, whiskers, and graphite polyhedral crystals (GPC) [13] are built from the same graphene sheets as bulk graphite (Fig. 1), they are often considered separately from graphite [14].

S. Rotkin  
Beckman Institute, University of Illinois at Urbana-Champaign,  
Urbana, IL 61801, USA

Y. Gogotsi (✉)  
Drexel University, Department of Materials Engineering,  
3141 Chestnut St., Philadelphia, PA 19104, USA  
e-mail: gogotsi@drexel.edu  
Tel.: 215-895-6446, Fax: 215-895-6760

Graphite has been thoroughly studied and information about its structure and properties is easily available. In particular, basal planes of graphite have received much attention. Graphite edge planes have been studied to a lesser extent and the dominating opinion is that “the dis-

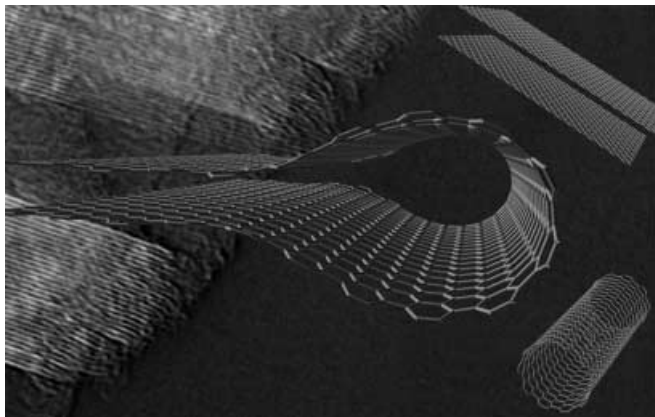
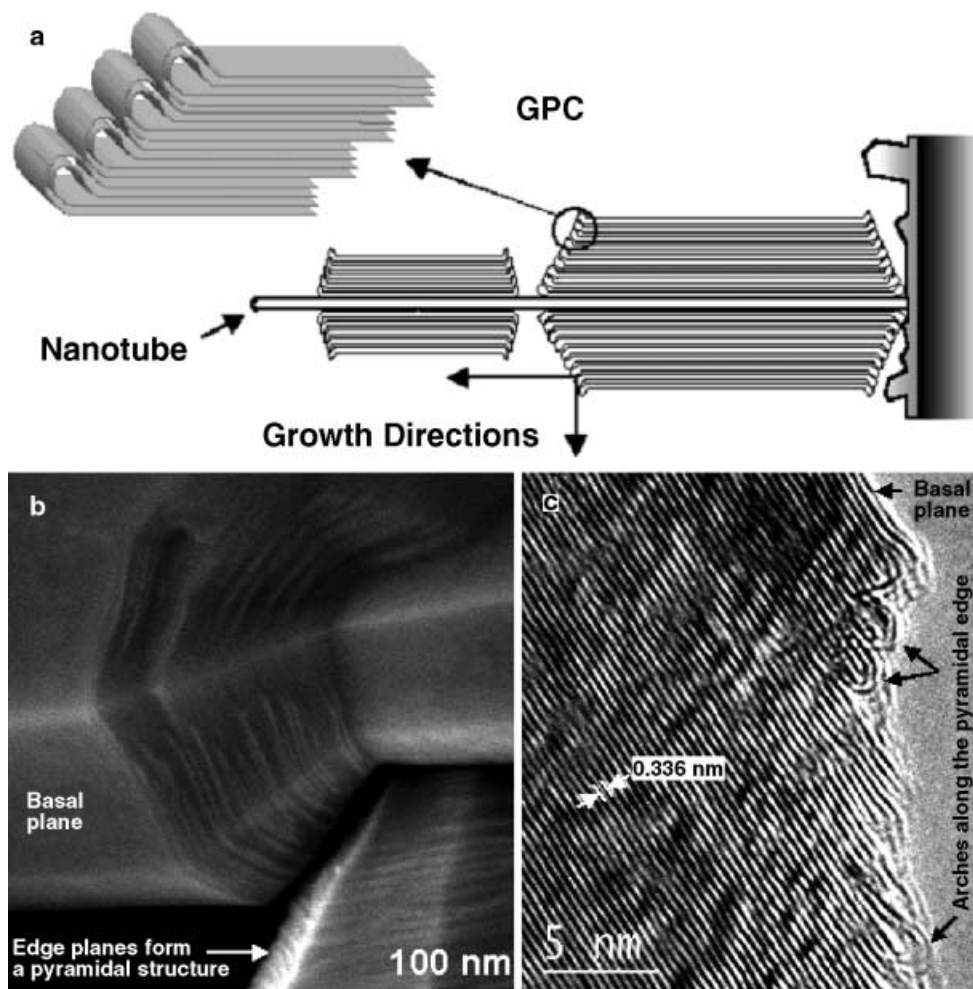


**Fig. 1** The molecular dynamics (MD) simulation result for the zipping of the graphene edge. Similarities between a sleeve formed at the edge of graphite and an armchair single-wall carbon nanotube can be clearly seen. The picture in the background is a TEM image of a GPC edge

**Fig. 2** (a) Schematic showing the suggested mechanism of GPC growth around a carbon nanotube core; (b) SEM micrograph of pyramidal surfaces of two GPCs and (c) TEM micrograph of a GPC tip showing arches formed by folding graphene sheets

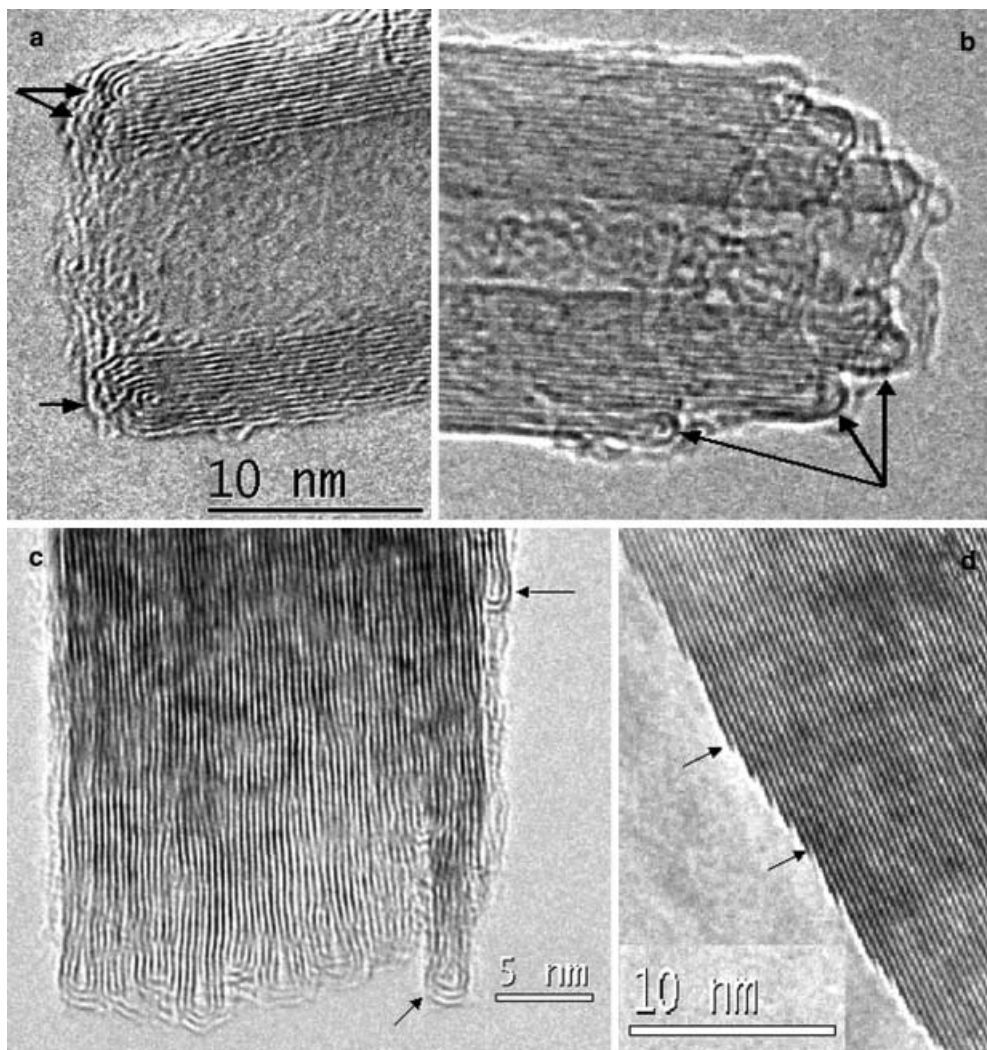


continuity of graphite planes inevitably exists at the edge” [8]. Surface reconstruction is known to be extremely important for Si, the material of 20th century electronics. However, surface reconstruction has been much less studied for graphite. One of the reasons might be graphite’s limited use in electronics because fabrication of ordered graphite substrates is difficult. This work shows that interesting perspectives could be explored by studying the mechanisms of the edge reconstruction of different graphitic materials. Both experimental results and a model of the graphite edge structures will be presented in this work as shown in Fig. 1, and a general approach to describe non-planar graphite (nanotubes and similar structures) will be demonstrated.

### Relation to previous work

Recently novel polyhedral nano- and microstructures with the shapes of faceted needles, rods, rings, barrels, and double-tipped pyramids (Fig. 2) were discovered [13], [16]. They represent a new class of carbon materials having nanotube cores, nanotube-structured tips, and graphite faces. These crystals bridge a gap between the

**Fig. 3** TEM micrographs showing tips of open carbon nanotubes (a) produced by hydrothermal synthesis below 800 °C and (b) grown within pores of glassy carbon at 2000 °C; (c) flake of natural graphite (Alfa Aesar), and (d) an inner wall of a carbon microtube produced by hydrothermal synthesis at 800 °C. Different number of graphene layers and folded structures in the walls of the tube shown in (a) imply a non-cylindrical (polyhedral) shape of the tube. Arrows show edge termination of graphene planes. Note differences in plane termination in (c) and (d)



nanotubes and planar graphite [13]. Their crystal habit, which can be axially true or helical, is derived from the core carbon nanotube and some of them are radially extended polyhedral nanotubes (Fig. 2). They were named graphite polyhedral crystals due to their perfect structure and continuous graphene layers [13]. A typical feature of these crystals is a presence of continuous nano-arches on the pyramidal edge planes (Fig. 2). These arches result in a swelling of the edge planes (Fig. 2a, b) and pyramidal growth occurs to accommodate the loops as can be seen in Fig. 2b.

Analysis of other graphitic materials has shown that these edge structures are very common. They have been observed in graphite filaments [17], multi-wall carbon nanotubes (MWNT's) (Fig. 3a, b), carbon cones [18], synthetic [19] and natural graphite (Fig. 3c). Moreover, these arch-shaped edges were formed in a very broad range of growth temperatures and environments (Fig. 3). Manipulation using a tip of a scanning probe microscope (SPM) was shown to result in the scrolling of the edges of graphite [20–22] leading to similar tubular structures. Graphite thus commonly shows a scrolled structure as

compared to atomic steps, which are common to surfaces of other crystals. In graphite, we only observed steps (Fig. 3d) on surfaces grown in highly reactive hydrothermal environments, where bent graphene layers, having a higher energy, could be attacked and dissolved while radicals were attached to the edge decreasing its free energy. However, even under these harsh growth conditions, loop formation has eventually been observed (Fig. 3a).

Typical arches that we found in GPC's and graphite crystals were built by folding two graphene layers (Fig. 2a). Sometimes, the number of layers increased to three or four (Fig. 3) and often a non-terminated layer of graphite was enclosed between the folded layer(s). Single folded sheets have been found as well and they always ended with an arch (Fig. 2c). In cross-section, these folded layers look like semi-tubes and are expected to show some of the vibrational and electronic properties of nanotubes. A possible Raman mode of the fine edge structure for GPCs has been observed in the spectra taken from GPC tips [13]. At the edge of graphite crystals, space quantization effects and quantum effects,

owing to the nanosize structural features, may develop. These edge structures may have electronic properties between the one-dimensional nanotubes and the layered graphite and an investigation of their properties should be undertaken. Other graphite-like materials, such as hexagonal boron nitride, demonstrate a very similar edge termination [18].

Based on available TEM data, we believe that a common mechanism governs the growth of such graphitic structures as macroscopic graphite crystals, microscopic GPCs and nanoscale carbon tubes and cones. Close similarity between the morphology of the natural reconstructed dangling bonds at the pyramidal surfaces of GPCs (Fig. 2) and the SPM-stimulated scrolls of the graphite edges [20, 21] leads us to the conclusion that nanotube-like zipping of graphite faces describes the dominant mechanism of edge termination of graphite. Thus, a unified approach can be used to describe the growth mechanisms of nanotubes and graphite.

### Unified approach to energetics of graphitic systems

Description of the transformation of planar graphene sheets into curved surfaces is the main goal of this paper. The rolling is not normally possible in the bulk because this process is always related to generation/recombination and motion of existing lattice defects, which is hindered by a low mobility of carbon atoms in the graphite lattice (or within a graphene layer). In contrast, the rolling occurs easily at the surface. That ties the modeling of the surface of micro- and macro-systems (which are to be considered as the bulk graphites in all other respects) to the simulation of nanoclusters of finite size.

We use a rather simple continual model of graphitic systems, which is motivated by the clarity of the obtained results and a unique possibility to compute the formation energies for almost any cluster or crystal modification on the same theoretical basis. Although other methods were used for calculating the formation energies of graphite and related materials, including an *ab initio* calculation of the total electronic energy of clusters and a subsequent minimization over various configurations, they are time-consuming and have only been applied to selected clusters. This non-empirical computation for a system including more than a hundred atoms is rather complicated. Several successful works which used tight-binding modeling were published on some specific shape clusters of larger size [23].

### Four-parameter model

A phenomenological continual model was developed by one of us for calculating the formation energies of carbon nanoclusters (CNC) with a curved graphitic surface [24, 25]. The model possesses enough flexibility to put forward a common foundation for the simulation of any planar or curvilinear system with morphology close to

graphite. The principle which allows us to develop a unified theory, is based on the expansion of the total formation energy of the system in a series. It has been shown [26, 27] that there are four approximately independent energy components, as well as a large constant contribution which is the chemical potential of the carbon atom in a flat graphene. Henceforth, we will count the energy from the “zero level” of the infinite graphene sheet and omit this large ( $\sim 7$  eV/atom) constant. Then, four contributions to the total energy can be written as:

$$E = N_d \varepsilon_d + \frac{N_6}{K(R_1, R_2)} E_c + N_b E_b + N_{cont} W \quad (1)$$

where  $N_d$  is the number of defects (primarily pentagons and heptagons) in the hexagonal lattice of graphite or CNC<sup>1</sup>. It equals zero for the perfect graphite lattice. The defect energy,  $\varepsilon_d$ , consists, in general, of two parts: the dislocation (disclination) core energy and the elastic energy accumulated in the distorted lattice around the defect. The latter is accounted for separately in the second term. This term is parametrized with the characteristic elastic energy  $E_c$  (the elastic tensor, in general case) resembling the flexural rigidity of a thin shell, as discussed in Refs. [24, 29, 30, 31]. Any external stress should be included in Eq. (1) explicitly, but we do not consider it here. The tensor of curvature  $K(R_1, R_2)$ , where  $R_1$  and  $R_2$  are the principal radii of the curvature [32], defines the internal strain. Therefore, the whole second term diminishes to zero for the perfectly flat graphite structure. This term collects all elastic contributions and counts all atoms in hexagons,  $N_6$ , except the ones belonging to the defects or to the system edges. The surface energy (third term) is modeled at the microscopic level by counting the number of dangling bonds,  $N_b$ , multiplied by the dangling bond energy,  $E_b$ . This characteristic energy can vary with the change in the surface bond population. A quantum chemical study is required to obtain the value for  $E_b$ . In many cases the edge reconstruction and bond rehybridization do not exist and our energy calculation is straightforward, but it is not restricted to a free non-passivated surface. It is an open question what is the surface energy of graphene. We consider the  $E_b$  as a phenomenological parameter, which adds flexibility to the model. The fourth term (van der Waals energy) is roughly proportional to the number of neighbor atoms in the adjacent layers,  $N_{cont}$ . Graphite, its modifications, and other layered crystals are described within the van der Waals theory in respect to the interlayer interaction energy,  $W$  [31, 33]. These interaction forces are essentially short ranged which justifies the use of the simplest approximation of the contact interaction<sup>2</sup>.

<sup>1</sup> The number of defects relates to the total Gaussian curvature of the surface and, for purely topological reason, it cannot be neglected in many cases. For example, according to Gauss-Bonnet theorem, any closed spheroid has 12 pentagons and an arbitrary number of hexagons [28]. For the same reason, a single pentagonal defect never appears in the lattice of planar graphene.

<sup>2</sup> The multi-body correction to this last term can be made using the dielectric function approximation but it goes beyond the article limits. We will discuss it elsewhere.

The four characteristic energies of the model were selected to fit to the results of the experiment and computer simulation. The appropriate values for the energies, taken from Refs. [25–27, 34], are:  $\epsilon_5 \sim 1.5$  eV (for the pentagon core),  $E_c \sim 0.9$  eV/ $b^2$  (bond length  $b \sim 0.14$  nm),  $E_b \sim 2.36$  eV (without passivation, rehybridization or any edge reconstruction<sup>3</sup>), and  $W \sim 35$  meV/atom. The formation energy of any cluster of a specified geometry can be defined using these values. The optimization of the geometry is understood as the minimization of the energy, given by Eq. (1), by the variation of the cluster shape at the fixed number of atoms, which tolerates neglecting the chemical potential term.

The model used here combines the quality of the atomistic approach with the simplicity of the continuum mechanics. This is provided by the lowest order expansion of the total energy at small curvature and defect density, which are the only relevant parameters in our case. Formally, the model equations are close to the continuum thermodynamics, that one must expect for such a linearization. However, the microscopic simulation has to be performed to match the characteristic energies, not just a simple adjustment to the continuum thermodynamics theory for the bulk material. With this caution, we call it the Continual Energetics (CE) model. Both MD simulation and analytical CE models give the shape and the formation energy of the optimal CNCs and the optimal shape of the edge structures for the surface reconstruction of the bulk material based on common principles. The optimal shape, which is the important aspect of this study, is in agreement by both theoretical approaches. Analytical results of CE are presented here because they are readily tractable and uncover the physics of the synthesis of planar and curved graphite.

---

### How energetics shapes the cluster

In the previous section, we introduced the CE model for the computing of the formation energy for the graphitic system supposing its shape is known. To calculate the most probable configuration, one considers an ensemble of systems of different shapes under quasi-equilibrium growth conditions; each system has a fixed number of atoms. The energy landscape minimum defines the area for the optimum structure locus in the configurational space of the relevant parameters. A locus of the minimum energy gives the optimum shape and morphology of the cluster. The characteristic formation energies are large compared with the typical thermal energy for synthesis which is less than 0.3 eV ( $T < 3000$  °K) and, therefore, the transformations between different configuration loci are kinetically suppressed. Hence, the system shape is given by the optimum parameters such as curvature, defect density, etc.

<sup>3</sup> It is known that the electronic structure of the carbon edge bonds can vary substantially [23, 35].

We assume that at least the initial step of the synthesis (the nucleation stage) occurs at the equilibrium. Under the growth conditions of GPC or graphitization of carbon, the whole synthesis is close to equilibrium and our model will predict the yield of the synthesis. Alternatively, the growth subsequent to the equilibrium stage might be limited by the kinetics. The initial nucleus shape cannot change as the temperature is low. Then, the nucleation energetics defines the morphology, and the kinetics defines the growth rates. Here, we restrict ourselves to the energetics only because we mainly address the nucleation.

The choice of system geometry under consideration, nanotube and nano-arch sleeve (Fig. 1), follows from the main objective of the paper: to trace the common features of the non-planar graphite formation. However, CE and MD simulations were performed in a wide range of geometries to define the optimum shapes of the different CNCs [24, 26, 27]. The important conclusion from this extensive study is that the system tends to diminish its surface energy, even at the expense of increasing curvature. Hence, we would expect the formation of the scrolled graphites to be a general behavior resulting from the natural ratio of the energetic parameters for the  $sp^2$  carbon. On the basis of the CE theory, the typical dimension of the self-organized features can be estimated from the analytical minimization of the total system energy.

The CE analysis predicts the optimum shape as the configuration delivering a conditional minimum to the function in Eq. (1) at the fixed geometry and the number of atoms. The calculation of the edge sleeve is similar to what has been done earlier for small CNCs, though it was simpler in the case of a high CNC symmetry. For example, the optimum shape of a planar flake (with or without pentagon defects) is close to a circle [26, 27, 36]. This shape has a minimum perimeter and, therefore, minimal surface energy (this is a continual result and we will discuss the correction to the edge shape below). In order to persevere in obtaining the analytical result for our edge structures, certain shape approximation will be made.

---

### Surface energy: zigzag edge orientation

The preferable edge orientation of the graphite is computed within the CE model. As will be discussed later, the orientation defines the specific edge reconstruction: the symmetry of edge arches, the presence or absence of defects, etc. The optimum edge orientation influences the coalescence and co-growth of coupled nuclei at the fixed angles (e.g., in GPC or polyhedral carbon particles), which will be discussed elsewhere.

The edge with the minimum density of dangling bonds has a minimum surface energy, not considering the reconstruction. For graphene, this is the zigzag edge. Indeed, the natural graphite flake has a hexagonal shape with the edges in [110] and symmetry equivalent zigzag

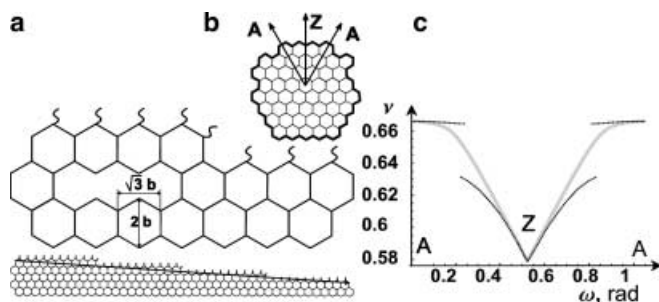


**Fig. 4** (a) The misoriented edge of graphite. The edge consists of a series of kinks. The thick line in the lower part depicts the continuum limit of the vicinal edge orientation. An enlarged view of a single kink is given in the upper part. (b) The view of a small graphite flake, which shows that no continuum edge geometry is possible on nanoscale, and a circular flake accepts a polygonal shape. (c) Dangling bond density,  $\nu$ , of the graphene edge vs. chirality angle,  $\omega$ . The surface energy of the graphene fragment is a periodic function of  $\omega$  because of  $\nu(\omega)$ . Dotted lines represent the linear approximations at the extremum points: A: armchair edge, Z: zigzag edge

directions [9], [37]. The misoriented graphene edge can be considered as a series of kinks (Fig. 4a) along the high symmetry direction. This allows us to calculate the edge surface energy depending on the edge misorientation angle. Similar to the free energy of 3D crystals [38], it has a cusp around the zigzag direction (minimum of the surface energy) and a parabolic shape around the armchair direction (maximum of the surface energy), which is shown in Fig. 4c.

A closed expression for the surface energy of the graphite edge with an arbitrary orientation was presented in Ref. [39]. It is based on the assumption that the local hybridization at the edge does not vary with the edge orientation, which might not always be valid. For example, our model is not applicable to the chemically functionalized surface. We address an almost free graphite edge, which may be passivated. The typical energy gain due to one kink creation is approximately equal to the half of the dangling bond energy,  $E_b/2 \sim 1.2$  eV. This gives the scale of the energy needed to form the minimal misorientation of the edge. The formation energy of the misoriented edge is quite large compared to the synthesis temperature and, therefore, we must only consider zigzag edges at the equilibrium.

Let us now return to the assumption of the continual theory: the minimum of the surface energy corresponds to the minimal perimeter. In particular, a continuum planar flake will accept the circular shape. In reality, the density of bonds along the circular perimeter will oscillate (as shown in Fig. 4c) and will increase its contribution to the total energy given by Eq. 1.

CE model is easily modified to account for the actual lattice symmetry. The hexagonal lattice symmetry of graphene ( $D_{3h}$ ) is consistent with the properly (zigzag) oriented hexagonal fragment (the shape to be used instead of the circle, that was used above for the continual symmetry  $S_2 \equiv D_\infty$ ). Fortunately, it will not change the main CE model results for systems not containing pentagons, in particular, for the edge sleeve structure.

## Zippering of graphite edges

### Energetics of folding a graphene layer

Experimental evidence of the folding of graphite layers is presented in Figs. 1–3. Theory, describing folding of a single graphene layer, considers a free (not supported) monolayer which corresponds to suspended sheets of freshly cleaved graphite or to the manipulation of graphite layers with a mechanical probe (e.g., SPM tip). One needs a free monolayer to avoid consideration of the attractive van der Waals interaction between graphite sheets in the beginning of the process. However, we cannot neglect the van der Waals force completely, because it defines the shape of the final configuration. This was discussed earlier in context of the nanotube collapse (see Ref. [31]). The interplay between van der Waals and elastic energies results in the formation of the “sleeve” structure along the edge with its radius of curvature being independent on the length of the edge. It neither depends on the sleeve orientation (chirality), nor on the presence of defects. It means that the universal behavior can be predicted for the graphites from nanometer to millimeter scale.

Folding of graphene is not an energetically allowed process because it starts with the rolling and increase of the elastic energy of the layer. The rolling of a graphene rectangle, resulting in closing of the dangling bonds at the opposite edges, is known to have a large energy barrier [40]. In the case of the edge folding, the final state has a lower energy owing to the van der Waals cohesion between the folded parts, but an external force is required to overcome the elastic energy barrier. After the top layer has touched the bottom one, the (negative) van der Waals cohesion energy of the system grows proportionally to the contact area between the parts decreasing the total energy of the system. Then the layers stick together and the sleeve diameter decreases until the increasing elastic energy balances the van der Waals cohesion.

The resulting structure has the diameter which is given by the ratio of the van der Waals specific energy to the elastic constant. For the parameters taken in the CE model, the optimum sleeve diameter is about 1.5 nm. The MD simulation<sup>4</sup> was done to refine the continual result which was confirmed qualitatively and was in good agreement with the experimental data (Figs. 2c and 3c) on the size of monolayer nano-arches in graphite. However, the optimum radius is slightly larger, being about 1.8–2.5 nm, which is within a typical range of diameters for SWNT’s. Thus, arches along graphite edges are predicted to have a curvature similar to SWNTs (Fig. 1).

<sup>4</sup> The commercial package Cerius2 (MSI software) was used to simulate structures of the size up to 3500 atoms. The Universal Force-Field [41] as well as Dreiding 2.21 [42] Force-Field were applied.

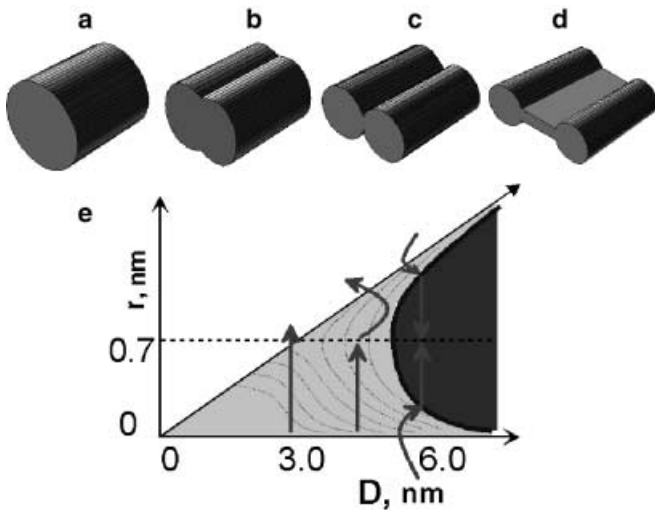


**Fig. 5** The stages of the nanotube collapse (a-d) and analysis of the sleeve creation on the graphite double-layer edge, showing the contour map of the energy landscape (e). (a) initial SWNT; (b) the sagged SWNT; (c) the pince-nez structure; (d) dumbbell structure with the sleeves formed at the edges. The optimum sleeve radius is about 0.7–1 nm. The coordinates plotted in (e) are the sleeve radius ( $r$ ) and NT diameter ( $D$ ). The collapse occurs at large NT diameters. At smaller diameters, the process goes in the opposite direction. SWNT's with the diameter larger than 5.5–6 nm are energetically metastable for the collapse. The intermediate-diameter SWNT's are more stable than the closed pince-nez structure, but the pop-up transformation has an energy barrier until the diameter of the opened tube becomes less than 3 nm. A thinner structure is unstable for the pop-up

### Nanotube collapse and recovery

The collapse of MWNTs has been experimentally observed [43, 44]. The van der Waals force is strong enough to cause the closing of a sagged nanotube of large diameter. We calculated the energy diagram for the collapsing process and demonstrated that the reverse process will be favorable in some regions which will be defined below analytically. Similar calculations were presented in Ref. [31] and the conclusion about stability of MWNT's of a certain diameter was drawn on the base of numerical computation. Let us consider the following path from a cylindrical SWNT (Fig. 5a) to the collapsed structure with two sleeves along the edges (Fig. 5d). In order to obtain an analytical expression within the CE model for the formation energy at each stage of the transformation, we had to simplify the shape of the intermediate "pince-nez" stage (c). In reality, all folds are smooth, though it does not change the qualitative CE result. The energy landscape has a complicated profile which changes with the SWNT diameter. For a sufficiently large diameter, the minimum energy is at stage (d), where the tube flattens and collapses. For a diameter smaller than  $D_c \sim 5.5\text{--}6$  nm, the energy minimum is in state (a), and the collapse is energetically suppressed. However, the states (a) and (d) are separated by an energy barrier, because the system energy has a maximum in the unstable pince-nez (Fig. 5c) and the final dumbbell

(Fig. 5d) stages. This is similar to the elastic energy barrier for the folding of flat graphene. The barrier decreases with SWNT diameter and disappears when it is smaller than 3 nm. These narrow pince-nez structures are unstable and tend to pop up, a process opposite to collapsing; thus, NT recovery is preferred. The diagram in Fig. 5e summarizes the results of this simulation. One can conclude that a thin double layer structure can serve as a seed for the SWNT nucleation. This may explain the formation of nanotubes in carbide-derived carbon (CDC) [45, 46].

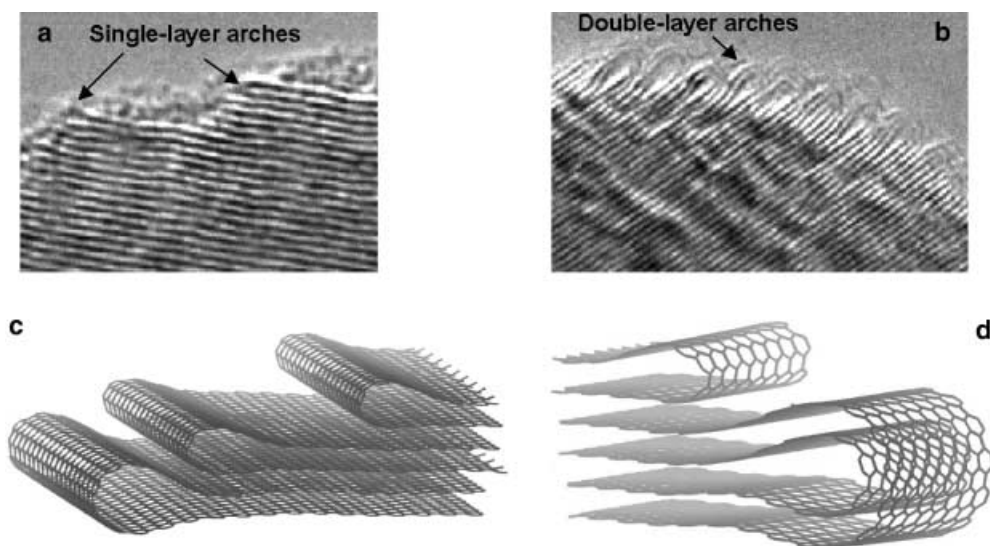
### SWNT nucleation by zipping

The double-sleeve pince-nez and dumbbell structures considered in the last section are shown to transform into SWNTs at small diameters. A similar conclusion can be made for each of the two edges: the sleeve opens and increases its diameter until the optimum geometry is reached. So, the flat closed double layer of graphite is recovered into the scrolled structure. While the structure in Fig. 5 is a hypothetical one, we propose to study the reconstruction of the real graphite edge (Fig. 6) to take into account the formation of tubular sleeves (which will be seen as arches in a cross-section) following closing of the dangling bonds along the edge. We call this SWNT nucleation mechanism "zipping" [27]. The zipping model does not cover every synthetic technique known for SWNT/MWNT production. However, it is useful for equilibrium growth and is interesting as a mechanism which is not involving pentagon formation and not requiring a catalyst explicitly. The role played by the catalyst metal particles in the formation of SWNT's was widely discussed in the literature [23, 47]. The effect of the dangling bond passivation and/or creation of complexes with transition metals can be incorporated into our model phenomenologically through the modified value of  $E_b$ .

Closing of the dangling bonds is energetically favored. If the edges of the closest graphene sheets are in registry, the "lip-lip" bond formation is allowed [47], [48] and a perfect nanotube-like structure grows, whereas incommensurate edges form a sleeve, which inevitably contains defects. After the new bond formation, the edge is still far from equilibrium. The bond angles and lengths are not the same as for planar graphite. To release this elastic energy, the edge has to pop up and form a wider sleeve. However, this costs additional energy because the van der Waals cohesion will be lost in the sleeve wall area. Finally, the sleeve arrives at equilibrium with the minimum energy. The CE calculation shows that the optimum circular sleeve diameter is determined by the ratio of the elastic constant to the van der Waals specific energy [49]. The CE analytical result reads as:

$$D_o = 3b \sqrt{\frac{E_c}{2W}}. \quad (2)$$

**Fig. 6** TEM micrographs of GPC edge structures (**a, b**) and MD simulation output (**c, d**) for multiple layer folding with a single (**a, c**) and double (**b, d**) layers involved in the arch formation. The system modeled mimics the graphite or GPC edge structure in respect to the existence of the multiple layers and the sleeves formed at the open surface. The radius of the sleeve along the closed edge depends on the geometrical constrictions, which are by the angle of the edge plane



The MD simulation was performed to confirm the continual result. The optimum diameter is  $\sim 2$  nm but the shape is not very close to the semi-circular one (Fig. 1).

As we discussed, the edges meeting in registry will form a half-nanotube sleeve, but only two graphene edge orientations allow a defect-free zipping. Namely, the zigzag and armchair edge orientations lead to the creation of the armchair and zigzag SWNT arches respectively (note that the tube and edge orientations are complementary). The zipping formation of the zigzag arch is suppressed for energy reasons owing to high surface energy of the armchair edge. This also explains qualitatively the preferable formation of armchair SWNT's [50].

### Graphite edge reconstruction

The process of graphite edge reconstruction is very similar to the sleeve formation considered in the previous sections. Two other complications are considered: (I) the van der Waals interaction between different sleeves affects their shape and (II) a geometrical constriction appears depending on the orientation of the crystal surface in the direction normal to the reconstructed edges. Both, hexagonal and rhombohedral graphite have been considered. Since both modifications show very similar behavior, we present here results for hexagonal graphite. A similar simulation can be performed for the graphite-like hexagonal BN lattice.

The van der Waals interaction between graphene sheets results in either (1) the formation of single-wall (Fig. 6c) and double-wall (or multi-wall) sleeves (Fig. 6d), or (2) in deformation of the existing sleeves. Both are consistent with the processes during nanotube formation. They resemble the growth of (1) MWNTs and (2) SWNT-ropes, respectively. The shape of the deformed sleeve does not exactly have a three-fold symmetry, as it appears for the inner tubes in the ropes, where a triangular superlattice forms [51]. Instead, it has a circu-

lar quadrant cross section because one of its sides enters the free surface (Fig. 2a).

One would expect that the formation of a pyramidal (Fig. 2) or jigsaw facet is energetically favorable compared to a straight facet without reconstruction. This is because the optimal diameter of the sleeve is larger than the available interlayer distance (0.335 nm). This geometrical constriction affects the surface diffusion-limited growth. The sleeve along the reconstructed edge has different atomic friction properties than a simple lattice kink. Hence, the edge transformation of the underlying layer might induce total facet reconstruction at a given angle, which is determined by the sleeve dimensions.

The preferred (zigzag) edge orientation and faceting, which is controlled by the edge reconstruction, define together the specific conditions of the polycrystalline growth. This growth will result in the high degree of mutual orientation of neighbor domains.

It is necessary to mention that the multiple layers of the curved structures are not commensurate even if the initial graphene sheets were. The incommensurate structure results in a nontrivial dependence of the interlayer interaction energy on the geometry and a low-symmetry allotrope can form.

### Potential applications

Numerous applications for the nano-arches (nanotube-like edge structures) may appear due to the high extent of orientation and uniformity provided by the self-organized growth mode. Non-crystallographic edge planes of graphite may exhibit low friction coefficients predicted for nanotubes and unusual electronic properties. Inter-arch cavities at the edge of the graphite crystal or GPC can be occupied with dopants that cannot fit between graphene layers, because fairly large atoms can be accommodated under the arch. Thus, intercalation with larger atoms, organic molecules, atomic clusters and

even 1D crystalline nanowires should be possible. Li-ion intercalation through the nano-arches produced high battery performance with a large discharge capacity and a small irreversible capacity [19]. Having a large similarity to nanotubes, the pyramidal facets of GPC's can serve as ideal substrates for ordered NT synthesis.

The superb mechanical stability of the closed carbon edge may be accompanied with a nontrivial modification of its electronic structure. A wide range of behavior, ranging from high-temperature superconductivity [52] to ferromagnetism [53], has been shown experimentally to exist in graphitic materials. The origin of this variety of properties is in the unique electronic structure of the 2D hexagonal lattice of graphite. Unlike other conductors, it only has Fermi-points instead of a Fermi-surface. The mobility of these points under external influence can result in essential changes in the macroscopic electrical properties. Its responsiveness to mechanical force (changing the local symmetry of the graphite) gives promise to engineering the electronic properties by controlling the morphology.

Since graphite edge reconstruction favors the zigzag configuration of tubular edges, arrays of armchair "semitubes" are formed along the edges. Since the control over the structure and chirality of free standing SWNTs and MWNTs is a problem, nanoarches may offer controllable tube arrays with a given structure, which determines the electronic properties. However, similar to nanotubes produced by current synthesis techniques, edge structures have a variety of diameters and, typically, from one to four graphene layers are found within a single edge sleeve, but more than a dozen of layers similar to MWNTs were observed in synthetic graphite [19]. The effect of the growth process variables on the edge structure should be investigated to gain control over the sleeve size distribution.

## Conclusions

Graphite and hexagonal boron nitride crystals have zipped edges forming nano-arches. A new unified theoretical approach, developed to understand this behavior, bridges the gap between descriptions of planar graphite and nanotubes.

We have demonstrated that the CE model supports the experimental fact that the most energetically stable free surface of graphite has a zigzag orientation. The edge nano-arch structures are shown to have a preferable armchair orientation (complementary to the free zigzag edge).

The folding of graphitic carbon has been theoretically studied. Transition to curved surface happens equally at different scales and for different materials. For example, hexagonal and rhombohedral graphite, as well as hexagonal BN crystals, have nanotube-like features along their edges.

A sleeve at the edge of graphite is predicted to have the optimum diameter,  $D_o$ , of 1.5–2 nm. The diameter depends neither on the edge structure, nor on the defects

or contamination of the graphite. It is solely defined by the van der Waals cohesion and the elastic energy of the rolled graphene layers.

Simulated sleeve/cylinder structures, which diameters differ from  $D_o$ , can undergo the flattening or recovery of their cylindrical shape depending on whether  $D$  is larger or less than  $D_o$ .

Tendency of graphite to form curved edge structures may be a main reason why graphite single crystals are rare and can only be grown from liquid metals or mineral melts, when etching of edges prevents zipping of graphene planes.

Passivation of graphite edges due to the reconstruction and plane zipping is expected to complicate the functionalization of graphite edges. Opening of the closed graphite edges may be required for efficient intercalation of graphite. Etching, oxidation or mechanical damage can open the graphite structure by removing the zipped edges.

Unique electronic and mechanical properties of nano-arch edges, which form arrays of semitubes, are expected and may be attractive for nanotechnology applications.

**Acknowledgements** This work was supported by the US Department of Energy, grant DE-FG02-01ER45932. S.V.R acknowledges the Beckman Fellowship from the Arnold and Mabel Beckman Foundation. Y.G. is thankful to his former students at the University of Illinois at Chicago Mr. Joseph A. Libera and Mr. Nikolai Kalashnikov for experimental help. Thanks are also due to Mr. Ethan Hackett, Drexel University, for his comments on the manuscript and to Mr. Benjamin Grosser, ITG, Beckman Institute, University of Illinois at Urbana-Champaign, for help with the design of Fig. 1.

## References

1. Kroto HW, Heath JR, O'Brien SC, Curl RF, Smalley RE (1985) *Nature* 318: 162–163
2. Iijima S (1994) *MRS Bull.* 19: 43–49
3. Schon JH, Kloc C, Batlogg B (2000) *Nature*: 702–704
4. Antonov RD, Johnson AT (1999) *Physical Review Letters* 83: 3274–3276
5. Crone B, Dodabalapur A, Lin Y-Y, Filas RW, Bao Z, Laduca A, Sarpeshkar R, Katz HE, Li W (2000) *Nature* 403: 521–523
6. Martel R, Schmidt T, Shea HR, Hertel T, Avouris P (1998) *Appl. Phys. Lett.* 73: 2447–2449
7. Tans SJ, Verschueren ARM, Dekker C (1998) *Nature* 393: 49–52
8. Inagaki M (2000) *New carbons: control of structure and functions* (Elsevier)
9. Endo M, Saito R, Dresselhaus MS, Dresselhaus G (1997) *From carbon fibers to nanotubes*, in *Carbon Nanotubes*; Ebbesen TW, Ed. (CRC Press, Boca Raton) pp. 35–110
10. Bacon R (1960) *J. Appl. Phys.* 31: 283–290
11. Iijima S (1991) *Nature* 354: 56–58
12. Schlittler R R, Seo JW, Gimzewski JK, Durkan C, Saifullah MSM, Welland ME (2001) *Science* 292: 1136–1139
13. Gogotsi Y, Libera JA, Kalashnikov N, Yoshimura M (2000) *Science* 290: 317–320
14. Harris PJF (1999) *Carbon nanotubes and related structures* (Cambridge University Press, Cambridge)
15. Gogotsi Y, Libera JA, Güvenç-Yazicioglu A, Megaridis CM (2001) *In-situ fluid experiments in carbon nanotubes*, In *Materials Research Society Proceedings (MRS, Boston)* Vol. 633: pp. A7.4.1–A7.4.6

16. Gogotsi Y (2001) *Crystal Growth and Design* 1: 179-181
17. Murayama H, Maeda T (1990) *Nature* 345: 791-793
18. Bourgeois L, Bando Y, Kurashima K, Sato T (1998) Boron nitride/carbon cones and ring defects, In *International Symposium on Carbon* (Tokyo, Japan) pp. 60-61
19. Moriguchi K, Munetoh S, Abe M, Yonemura M, Kamei K, Shintani A, Maehara Y, Omaru A, Magamine M (2000) *Appl. Phys. Lett.* 88: 6369-6377
20. Roy H-V, Kallinger C, Marsen B, Sattler K (1998) *Journal of applied physics* 83: 4695-4699
21. Roy H-V, Kallinger C, Sattler K (1998) *Surface Science* 407: 1-6
22. Atamny F, Fassler TF, Baiker A, Schlögl R (2000) *Applied Physics A: Materials Science & Processing* 71: 441-447
23. Lee YH, Kim SG, Tomanek D (1997) *Physical Review Letters* 78: 2393-2396
24. Rotkin VV, Suris RA (1995) Carbon cluster formation energy, In *fullerenes. Recent advances in the chemistry and physics of fullerenes and related materials*; Ruoff RS, Kadish KM, Eds. (Electrochemical Society, Pennington, NJ) vol. PV 10-95: pp. 1263-1270
25. Rotkin VV, Suris RA (1998) *Energetics of fullerene cluster* (Mater Res Soc., Warrendale) pp 175-180
26. Rotkin SV, Suris RA (1999) *Phys. Lett. A* 261: 98-101
27. Rotkin SV (2000) On energetics of nt nucleation through zipping of carbon layer edge, In *Fullerenes 2000, volume 10: chemistry and physics of fullerenes and carbon nanomaterials*; Kamat PV, Guldi DM, Kadish KM, Eds. (ECS Inc., Pennington, NJ) vol. PV 2000-12: pp. 66-71
28. Kozyrev SV, Rotkin VV (1993) *Sov. Semiconductors* 27: 777-791
29. Robertson DH, Brenner DW, Mintmire JW (1992) *Phys. Rev. B* 45: 12592-12595
30. Nardelli MB, Yakobson BI, Bernholc J (1998) *Phys. Rev. B* 57: R4277-4280
31. Benedict LX, Chopra NG, Cohen ML, Zettl A, Louie SG, Crespi VH (1998) *Chemical Physics Letters* 286: 490-496
32. Korn GA, Korn TM (1961) *Mathematical handbook for scientists and engineers*; (Mcgraw-Hill Book Company, Inc., New-York)
33. Girifalco LA, Hodak M, Lee RS (2000) *Physical Review B* 62: 13104-13110
34. Rotkin VV, Suris RA (1996) *Molecular Materials* 8: 111-116
35. Nakada K, Fujita M, Dresselhaus G, Dresselhaus MS (1996) *Physical Review B* 54: 17954-17961
36. Rotkin SV, Suris RA (1998) The bond passivation model for carbon nanoparticle growth, in *International Symposium Nanostructures: Physics and Technology*, St. Petersburg, Russia) pp. 335-338
37. Ager III JW (1995) *Mat. Res. Soc. Symp. Proc.* 383: 143-151
38. Wulff GS (1901) *Z. Kristallogr Mineral* 34: 449-530
39. Rotkin SV (2001) On surface energy of graphene and carbon nanoclusters, in preprint cond-mat/0107312
40. Lucas AA, Lambin PH, Smalley RE (1993) *J. Phys. Chem. Solids* 54: 587-593
41. Rappe AK, Casewit CJ, Colwell KS, Goddard WA, Skiff WM (1992) *J. Am. Chem. Soc.* 114: 10024-10035
42. Mayo SL, Olafson BD, Goddard WA (1990) *J. Phys. Chem.* 94: 8897-8909
43. Chorpá NG, Benedict LX, Crespi VH, Cohen ML, Louie SG, Zettl A (1995) *Nature* 377: 135-138
44. Crespi VH, Chorpá NG, Cohen ML, Zettl A, Radmilovic V (1998) *Appl. Phys. Lett.* 73: 2435-2437
45. Gogotsi YG (1997) Formation of carbon coatings on carbide fibers and particles by disproportionation reactions, in *NATO ARW: Advanced multilayered and fiber-reinforced composites*; Haddad YM, Ed. (Kluwer, Dordrecht), vol. 43: pp. 217-230
46. Kusunoki M, Suzuki T, Kaneko K, Ito M (1999) *Philosophical magazine letters* 79: 153-161
47. Charlier JC, Devita A, Blase X, Car R (1997) *Science* 275: 646-649
48. Kwon Y-K, Lee YH, Kim S-G, Jund P, Tománek D, Smalley RE (1997) *Phys. Rev. Lett.* 79: 2065-2068
49. Rotkin SV (2001) SWNT nucleation: energetics of zipping-edge mechanism, in *2001 symposium Mater Res. Soc. (Mater Res. Soc., Warrendale, PA) pp W2.9.1-W2.9.5*
50. Rotkin SV, Zharov I, Hess K (2001) Electronic properties of novel materials-molecular nanostructures (XVth International Winter School/Euroconference, Kirchberg, Austria, 3-10 March 2001) pp 454-457
51. Cowley JM, Nikolaev P, Thess A, Smalley RE (1997) *Chem. Phys. Lett.* 265: 379-384
52. Gunnarsson O (2000) *Nature* 408: 528-529
53. Kempa H, Kopelevich Y, Mrowka F, Setzer A, Torres JHS, Hohne R, Esquinazi P (2000) *Solid State Communications* 115: 539-542